Wind energy potential above a high-rise building influenced by neighboring buildings: An experimental investigation

Sarkic Glumac, Anina; Hemida, Hassan; Hoffer, Rudiger

DOI:
10.1016/j.jweia.2018.01.022

Document Version
Peer reviewed version

Citation for published version (Harvard):
Sarkic Glumac, A, Hemida, H & Hoffer, R 2018, 'Wind energy potential above a high-rise building influenced by neighboring buildings: An experimental investigation', *Journal of Wind Engineering and Industrial Aerodynamics*, vol. 175, pp. 32–42. https://doi.org/10.1016/j.jweia.2018.01.022

Wind energy potential above a high-rise building influenced by neighboring buildings: an experimental investigation

Anina Šarkić Glumac[a,*], Hassan Hemida[b], Rüdiger Höffer [a]

[a]Building Aerodynamics Laboratory, Ruhr-Universität Bochum, Universitätsstrasse 150, 44801 Bochum, Germany

[b]Department of Civil Engineering, School of Engineering, University of Birmingham, Birmingham B15 2TT, UK

Abstract

It is believed that the local topology has a significant effect on the wind flow pattern, wind velocity and turbulence intensity of the flow above the roof of buildings and thus is significantly influencing wind harvesting potential. This paper presents an experimental investigation, in which velocity field was measured above the roof of a high-rise building with a square cross section and height to width ratio of 1:3 surrounded by four buildings of the same geometry. In addition, the surface pressure was also measured. The flow above the roof was measured for different wind angles: 0°, 15°, 30°, and 45°. Results showed that there is a significant influence of the upstream building on the wind characteristics above the principal one. In general the wind angle of 45° is shown to be the most desirable angle for wind energy harvesting. The results of this work provide for the first time a database for the validation of computational fluid dynamic simulations for flat roof that will hopefully be used for more detailed investigations for urban wind energy harvesting.

1 Introduction

Renewable energy brings economic, environmental and social benefits to our community. One potential strategy related to energy is to maximize city's own energy generation of renewable energy and in the same way to minimize its impact on health and environment [1, 2]. In recent years, most of the wind energy was coming from flat terrain installations [3]. However, the urban environment has a potential for the wind power that has not been exploited [3, 4].

There are several advantages of harvesting wind energy in urban environment summarized in [3], such as the increased profitability of buildings, promoting the concept of zero-carbon building, the proximity to the consumption points enabling easier exploitation and the handy maintenance of wind harvesting devices. Nevertheless, the biggest disadvantage is related to the wind profile in urban environment as that is quite different from the classical log-law based profile [5, 6].

Due to large roughness length, the average velocity of the wind is lower in urban environments than over a flat terrain, where as the turbulence intensity is significantly higher [7]. These high levels of turbulence intensity are affecting the operability and the lifetime of wind turbines [7]. Therefore, wind turbines have to withstand a larger amount of fatigue loads that can affect the constructional design requirements of the wind turbines [8]. Thus, the turbulence intensity is an important factor that should be taken into consideration when wind harvesting is in question.

Despite existence of lower levels of average velocities in urban areas, regions with significant local high wind velocities are detected around and above buildings [1, 7]. For instance, such velocities can exist in the regions above separation bubbles that normally are formed above flat roofs of buildings [9]. This flow acceleration is evidently of great importance for the choice of the optimal location of the wind turbine. Taking into account that the energy given by the wind is a function of the third power of wind speed [7], wind turbines are best placed in areas where significant flow acceleration effect (speed up effect) is present.

Another parameter that can notably affect the amount of the energy harvested by the wind turbine is the skewness of the flow. The skew angle - the angle between the local velocity vector and the wind main direction - can significantly modify the amount of the energy harvested by the turbine. With this regard, there is an opposing behavior between Horizontal Axis Wind Turbines (HAWT) and Vertical Axis Wind Turbines (VAWT) [6] in terms of energy harvesting. While the HAWT's performance shows a decrease with increasing skew angle (for example, the power coefficient with an incoming flow of 15° inclination decreases on average by 7% [10]), recent works on Darrieus VAWT ([6, 11]) showed an increase in performance with regard to the skewed flow (the power coefficient with an incoming flow of 15° inclination increases by 20% [6]). In particular, this increase is observed for the attended angles in urban environment of 0°-30° [6]. Therefore, this flow characteristic could be significantly relevant for the choice of the turbine typology.

Locations of these desirable flow characteristics depend largely on the shape and the configurations of the surrounding buildings in the urban environment. Thus, it is important to carefully analyze flow pattern and its local wind characteristics around buildings in urban environments.

Related to the studies of wind flow in urban environment, many authors have focused their attention to the influence of adjacent buildings on wind-induced loads, taking into account different configurations. Namely, the studies covered assessment of the local wind loads on roofs and facades [12-17], as well as the impact of neighboring buildings on the overall structural loading [18, 19].

Other studies were concerned with the flow pattern developed around buildings. In particular, the flow pattern generated close to the edges of the roof for oblique wind directions has been well documented [20-24]. This pattern consists of two conical vortices, each associated with one of the upstream edges of the roof. Interest in such flow was raised due to the large wind loads as a consequence of high suction fluctuations caused by observed vortices. Mostly these studies are related to the isolated low-rise building. Although flow around isolated building has intensively studied in the past, the effect of upstream buildings on the conical vortices generated on the roof of a downstream building was not properly investigated [15]. In addition, all of those studies are focused on wind loading, in particular suction pressures, and not on urban wind energy harvesting.

When urban wind harvesting is in question, previous studies [1, 7] have addressed the effect of different roof profiles on both wind velocity and turbulence intensity. In these studies, four types of roofs were analyzed: flat, sloped, pitched and pyramidal roofs. In addition, [25] and [26] analyzed the flow above vaulted and domed roofs with lower turbulence characteristics. Besides considering different roof shapes, [1, 6] demonstrated interest on influence of building heights on the wind flow. Additionally, [6] assessed other general criteria as the height and the width of its upwind building and the distance between the buildings themselves, to evaluate the convenience of a microeolic turbine installation on the roof. All mentioned studies were based on the results of Computational Fluid Dynamics (CFD). These kinds of studies are essential for determining both the optimal location and the wind turbine model [3]. In [7] the power density available in flat, pitched and pyramidal roofs is assessed and it is concluded that the flat roof power density is greater and more consistent than above the other roof types. In [27], it was demonstrated that atmospheric boundary layer wind tunnel represents a reliable methodology for realistic estimates of urban wind energy potential. Two actual building cases in Montreal with different upstream roughness homogeneity were considered and results are compared with the corresponding field measurement data.

Despite the large number of CFD studies concerning wind harvesting potential, experimental data concerning urban wind energy potential is limited. Therefore, as part of the urban wind energy activities at the Building Aerodynamics Laboratory of Ruhr University Bochum (WIST), an experimental campaign of the wind flow around different types of buildings in different configurations was performed. This work was a part of the activities of the COST Action TU1304 [28]. The main aim of the presented work is to provide an improved understanding of the effect of the surrounding buildings on the flow characteristics over the roof of a high-rise building with respect to urban wind exploitation. Thus, local wind characteristics such as the flow pattern, local velocities, turbulent intensities and skew angle are analyzed. The data also provide a benchmark for the validation of Computational Fluid Dynamics (CFD) models aiming at the flow around high-rise buildings for the optimal location for installation of small wind turbines on the roof of buildings.

This paper is organized as follows: Section 2 refers to wind modeling and describes the wind tunnel facility, wind tunnel model, the instrumentation used for velocity and pressure measurements, Section 3 describes the main flow features above the roof of the building and the effect of the neighboring buildings in different configurations. The paper ends with conclusions in Section 4.

2 Experimental setup

2.1. Velocity profile

Wind tunnel experiments on a high-rise building model surrounded by four identical buildings were carried out in a Boundary Layer Wind Tunnel located at Ruhr University Bochum, Germany. The test section of the wind tunnel is 1.8 m wide and 1.6 m high. For this study, the flow of the atmospheric boundary layer in the wind tunnel was interpreted as a geometrical scale of approximately 1:300. The approaching flow represented an urban wind exposure using the spire-roughness technique. The mean wind profile matches that of a power law with exponent of 0.20 as shown in Fig. 1. The mean stream-wise wind speed (U), the stream-wise turbulence intensity (I_U) and the vertical turbulence intensity (I_W) at the height of the model were 16 m/s, 13% and 11%, respectively.

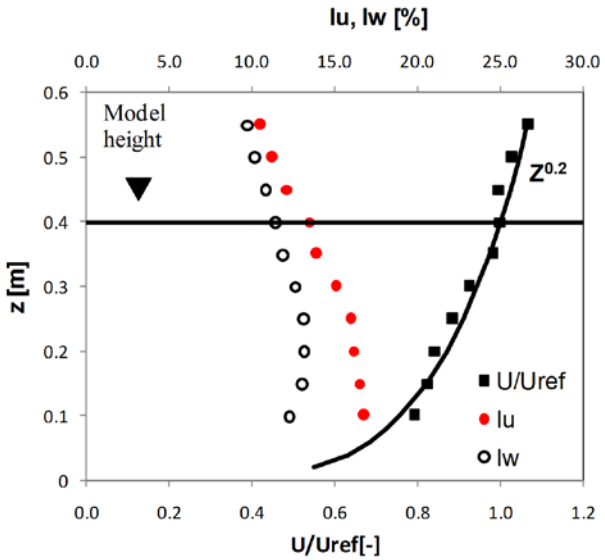

Fig. 1: Mean stream-wise wind speed (U/U_{ref}) ,stream-wise turbulence intensity (I_U) and vertical turbulence intensity (I_W) profile measured from the floor of the wind tunnel (U_{ref} is the mean wind speed at the model height).

2.2 Wind tunnel model and arrangement of buildings

The experimental model consisted of the principal building surrounded by four geometrically identical buildings. The geometrical arrangement is presented in Fig. 2.a). As shown in Fig. 2.b), the height of the building is denoted by *H* (400 mm) and the width by *D* (133.3 mm). The height to width ratio of the building was *H:D*=3:1. The roof is completely flat with sharp angles with the sides of the building. This configuration was investigated under four different wind angles: 0°, 15°, 30° and 45°. In each configuration, the flow characteristics above the roof of the principal building are compared to their levels at the referenced position at the height of the building in the undisturbed flow. The models mounted in the wind tunnel are presented in Fig. 2c).

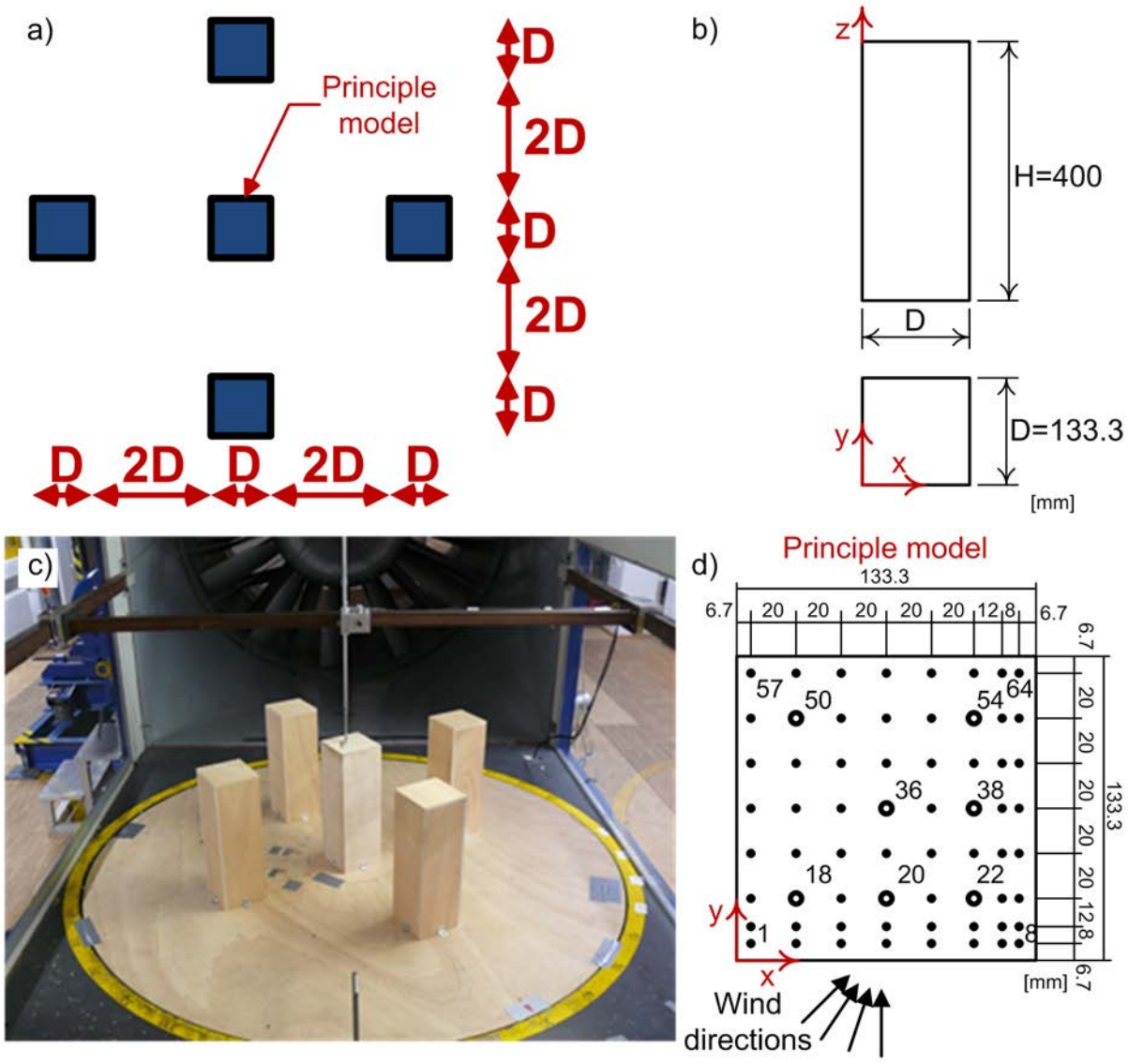

Fig. 2: a) Arrangement of the principal high-rise building (middle) surrounded with four buildings, b) model of the high-rise buildings, c) arrangement of the principal high-rise building surrounded by four buildings mounted in the wind tunnel, d) distribution of pressure taps on the surface of the flat roof (marked with ● and ○) and positions of velocity measurements (marked with ○) for 0°, 15°, 30° and 45° angle of flow attack.

2.3 Experiment procedure

Flow measurements were conducted using hot wire anemometry (a miniature X wire probe of DANTEC (55P61)). The velocities were measured above the points 18, 20, 22, 36, 38, 50 and 54 above the roof of the principal building, marked in Fig. 2.d). For that purpose, mainly three different heights (z/D= 0.075, 0.3 and 0.45) above the mentioned points were taken into consideration. The anemometer consisted of two cross wires allowing to measure two wind components in the stream-wise and the vertical directions. In order to minimize the impact on the flow field, only one hot-wire probe was used for all tests. The sampling frequency of the hot-wire probe was 2000 Hz. A Prandtl tube, mounted at the height of the model one meter upstream,

was used to set the reference wind tunnel velocity. Reynolds number based on the mean velocity at the height of principle building and the side of the roof was $1.4x10^5$.

The hot-wire anemometer has been calibrated in a laminar flow in a calibration tunnel by exposing the probe to a set of known velocities and corresponding voltages were recorded. The adopted fitting curve was a 4^{th} order polynomial curve with coefficients calculated by fitting the data in the least-squares sense. Uncertainties related to the velocity measurements were calculated following the procedure presented in [29] and [30]. The total uncertainty of the velocity was considered to consist of calibration, linearization, positioning of the probe, digitalisation and uncertainty due to variation of experimental conditions (such as temperature and ambient pressure). The maximum uncertainty of the time-averaged stream-wise velocity was 5.6%. The maximum uncertainties of the stream-wise and vertical turbulence intensities were estimated to be 9.6% and 9.4%, respectively. These uncertainty estimates correspond to 95% confidence interval. Due to the manual positioning of the hot-wire anemometer, uncertainty related to the positioning of the probe was detected as one of the main uncertainty contributors. It was established based on three repeated measurements at 10 different heights above the middle point of the flat roof.

Besides velocity measurements, surface pressures were measured at the roof surface of the principle building. The model was fitted with 64 pressure taps, presented in Fig. 2.d). The distribution of pressure taps on the flat roof of the principal building is shown in Fig. 2.d). Density of the pressure taps was increasing close to the windward sides of the roof. To measure the pressures at those positions, two types of pressure sensors were used: Honeywell 170 PC and AMSYS 5812-0001-D-B. Both sensors work by the same principle, by measuring differential pressures, expressed in voltage, between the pressures at the model surfaces and the static pressure of the Prandtl tube. Surface pressures were acquired with a sampling frequency of 1000 Hz using a multi-channel simultaneous-scanning measurement system. The maximum uncertainty of surface pressures based on 5 repeated measurements was estimated to be around 2.5%. Cut off frequency was 200 Hz. The pressure sensors were placed outside of the model and connected to the bores in the wooden deck by plastic pressure tubes with an inner diameter of 1.5 mm and a length of about 0.9 m. The tubing effects were numerically compensated [31].

In case of squat models (cubes) or prisms, [32] and [33] indicated that the upper bound for acceptable blockage is about 8-10%. Similar blockage limit set to 8% without adopting the correction, was used in work of [17] where the interference effect of prism buildings was analyzed and in [34] studying the pressure coefficients of low-tilted solar panels mounted on flat-roofed prism buildings. Thus, no blockage corrections of the measured results has been considered in this work, as even in the worst case the normal-to-wind areas of the testing models were smaller than 8% of the wind tunnel cross-section.

3. Results

3.1 Flow patterns

In this subsection, the profiles of the wind flow above the principal high-rise building, at four different flow angles: 0°, 15°, 30° and 45° are discussed. For comparison, velocity profiles are measured over the two lines: x/D=0.2 and x/D=0.8 considering the points 18-50 and 22-38-54 shown in Fig. 2.d). These profiles, based on stream-wise and vertical velocity component, are shown in Fig. 3. The position of these points is changing considering different flow angles. For example, points 18 and 50 are in the upstream half of the roof in case of large wind angles while

for small wind angles point 18 is in the upstream half and point 50 is in the downstream half. Similar observation is following second set of measurement points 22-38-54. Besides velocity profiles, Fig. 3 shows stream-wise (I_U) and vertical (I_W) turbulence intensities, obtained by:

$$I_U = \frac{\sigma_U}{U} \tag{1}$$

and

$$I_W = \frac{\sigma_w}{U}, \tag{2}$$

where σ_U and σ_W are standard deviation of stream-wise and vertical wind velocity components and U is the mean stream-wise wind speed. In addition, the percentage increase in the stream-wise wind speed related to the reference wind speed ($(U-U_{ref})/U_{ref}$) is also presented in Fig. 3, where U_{ref} is the mean referenced velocity measured by the Prandtl tube. All measurement results presented in this work are provided as Mendeley Data [dataset][35].

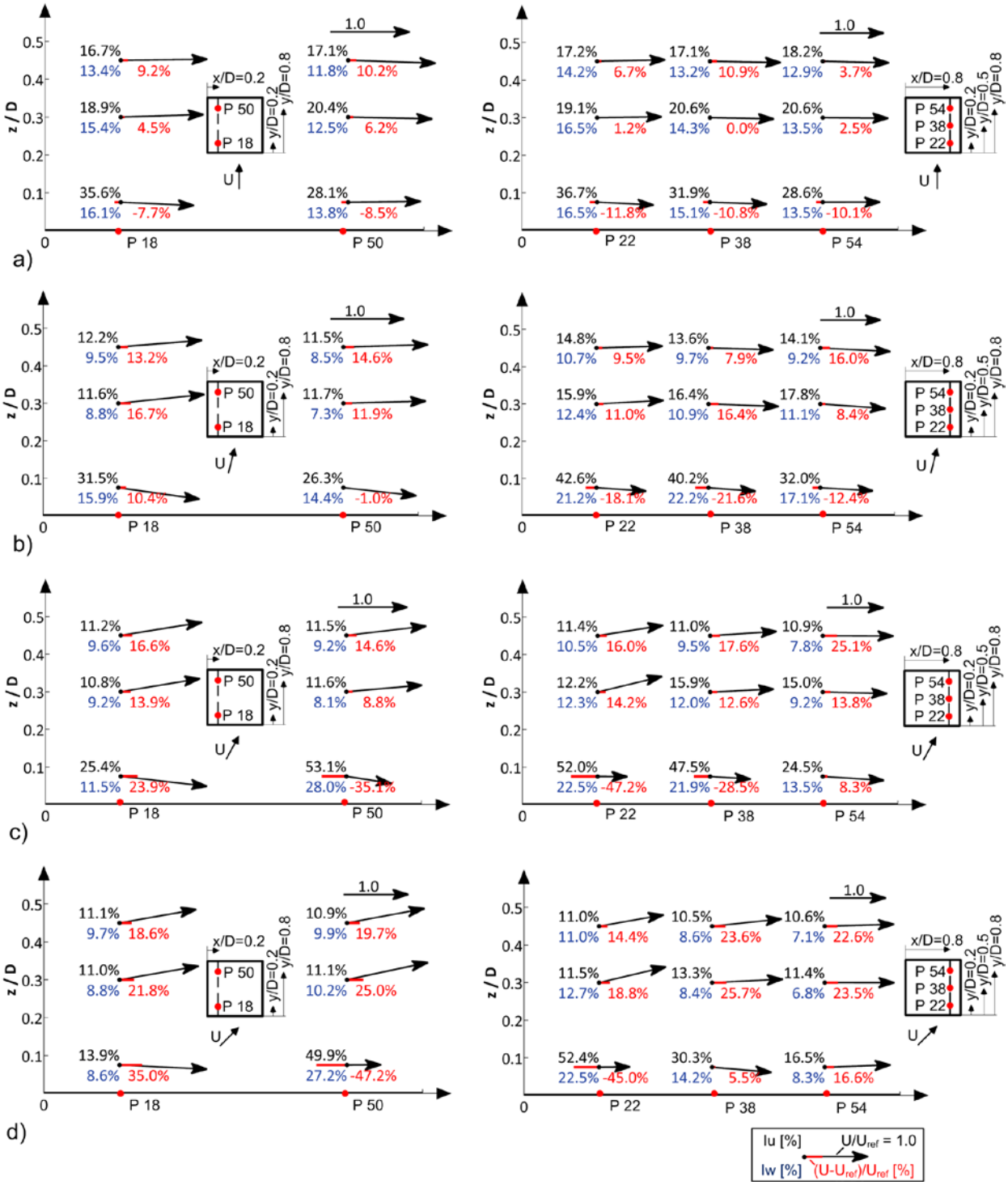

Fig. 3: Profiles of velocity vectors based on stream-wise and vertical velocity component, stream-wise turbulence intensity $I_{U,}$ vertical turbulence intensity I_W and percentage increase in the stream-wise wind speed. The legend linking the position of each value around the measurement point with its meaning indicates positions of : I_U - black number, marked left-up of the measurement point, I_W - blue number, marked left-down of the measurement point and percentage increase in the stream-wise wind speed - red number, marked right-down of the measurement point. Profiles over a principle high-rise building under the influence of 4 surrounding high-rise buildings are measured above the points 18 and 50 (belonging to

the marked line *x/D*=0.2, left) and above the points 22, 38 and 50 (belonging to the marked line *x/D*=0.8, right) for wind directions: a) 0°, b) 15°, c) 30°, d) 45°. The arrows indicate the velocity magnitude normalized with reference velocity (U_{ref}). Accompanying unity vector is represented in each plot.

For 0° wind angle, the mean wind flow is nearly parallel to the roof as almost all velocity vectors at higher positions above the roof (from *z/D*=0.3) are lacking vertical component (Fig. 3.a)). However, Fig.3. shows downward flow in the nearest vicinity of the roof meaning that the flow separates to form a small separation bubble close to the stream-wise edge. Rather high values of stream-wise turbulence intensities (I_U) are measured that are higher than 30%. In regions of such high turbulence intensity levels, hot-wire measurements are expected to be affected by some inaccuracies and therefore the results cannot be treated as reliable [29]. Nevertheless, these high values of turbulent intensity confirm the existence of separated flow.

In contrast to 0° case, the velocity profile for 15° wind angle is different, showing a formation of a small separation cone along the upstream side edge of the building. The velocity vectors at the lower measurement points along the line *x/D*=0.2, in particular above point 50, are pointing downwards. This suggests that the flow tends to attach to the roof. In near vicinity to the roof along the line *x/D*=0.8, high values of turbulence intensities are measured, suggesting the existence of separated flow.

The velocity profiles in case of wind angle of 30° indicate more pronounced upstream side-cone compared to 15° case. In addition, another separation cone is formed along the other upstream side of the building, affecting the flow above points 22 and 38. However, the flow over point 54 seems to be getting out of the influence of the separation cone. The lower measurement positions above points 22 and 38 are entirely in the separation zone as the turbulence intensity I_U is around 50%.

As in case of 30° wind angle, two conical vortices along the upstream edges are formed for 45° wind angle. Similar to the 30° case, the flow over point 54 is out of the influence of the separation cone.

The flow pattern above the roof can be analysed as well on the bases of the surface pressure. Fig. 4 shows contours of the mean surface pressure coefficient at the four measured wind angles. The pressure coefficient, C_p, is defined as:

$$C_p = \frac{p - p_\infty}{0.5\rho U_{ref}^2} \tag{3}$$

where p_∞, ρ and U_{ref} are the free stream pressure, air density and the reference velocity, respectively.

For 0˚ wind angle, a reduction in the surface pressure close to the upstream edge is directly followed by a build-up of pressure downstream. More pronounced reduction of the pressure close to the upstream corner is occurring in the case of 15º wind angle, suggesting large separation bubble. The other upstream edge is also showing similar behaviour only on the more confined area, confirming the existence of small side-cone. In case of high yaw angles of 30º and 45º very high reduction in surface pressures along both upstream edges is obtained. Here, the pattern of pressure distribution suggests that the flow separates at the upstream edges forming two intense conical structures, as observed from velocity measurements presented in Fig. 3. As expected, 45º wind direction provides a symmetrical case. From Fig. 4, it can be observed that the contour maps are very similar to each other when the wind direction varies from 15º to 45º.

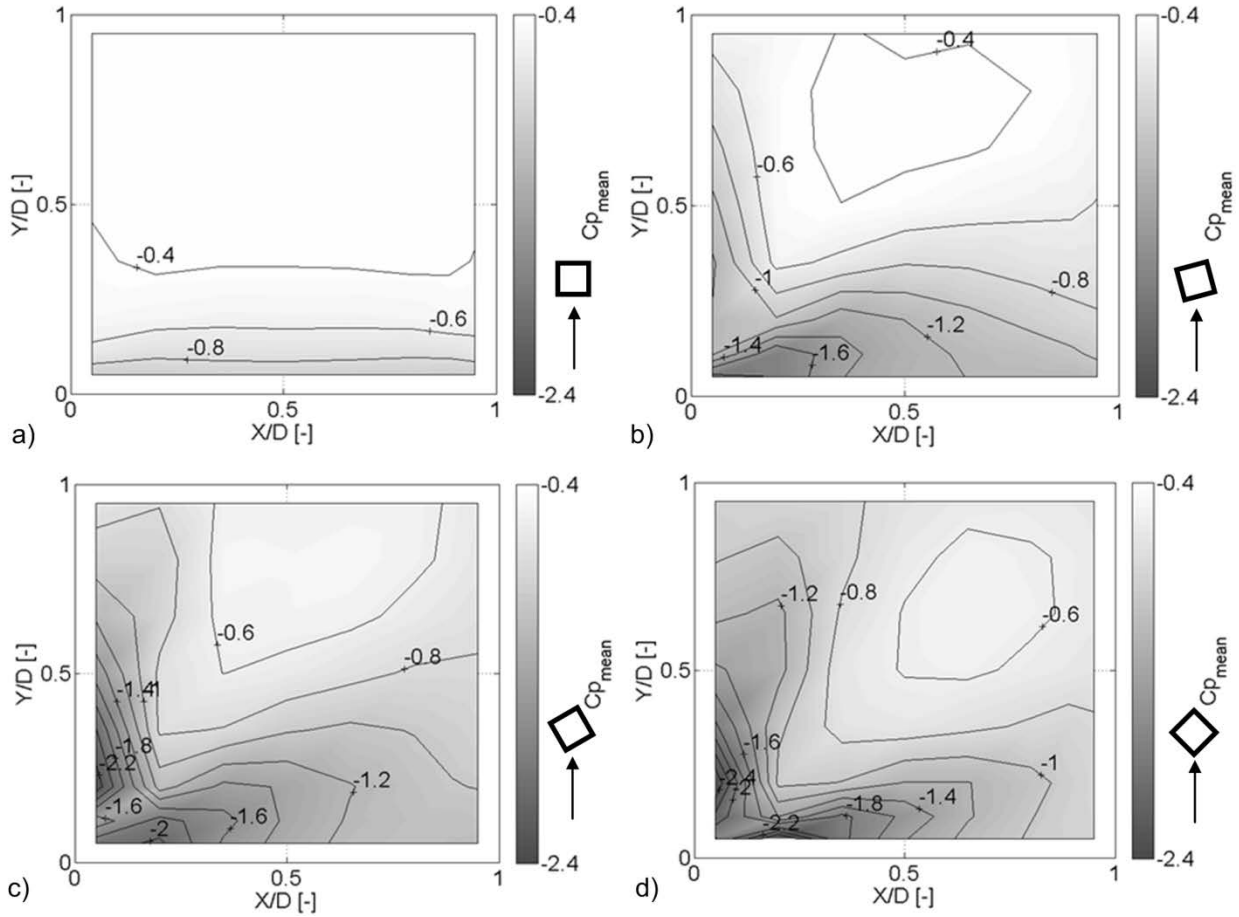

Fig. 4: Contours of $C_{p,mean}$ on the roof of the principal high-rise building under the influence of 4 surrounding high-rise buildings for different approaching flow angles: a) 0°, b) 15°, c) 30° and d) 45°.

In order to improve understanding of the effect of wind angle on the surface pressure, the mean pressure coefficient and its standard deviation have been plotted along two lines for different wind angles and shown in the Fig. 5. For wind angles of 15º, 30º and 45º, pressure coefficient distributions in Fig. 5 show similar pattern that is characterized with the upstream hump shape. This is typical for a flow with a separated region followed by a reattachment [36]. The hump shape is related to large negative pressure values in the separated region, where the largest suction was found directly beneath the average moving vortex core [23]. The length of the mean recirculation region is related to the peak location of the standard deviation value since the peak occurs just upstream of the mean reattachment position [36]. Therefore, the most pronounced separation is observed in case of 30º wind angle.

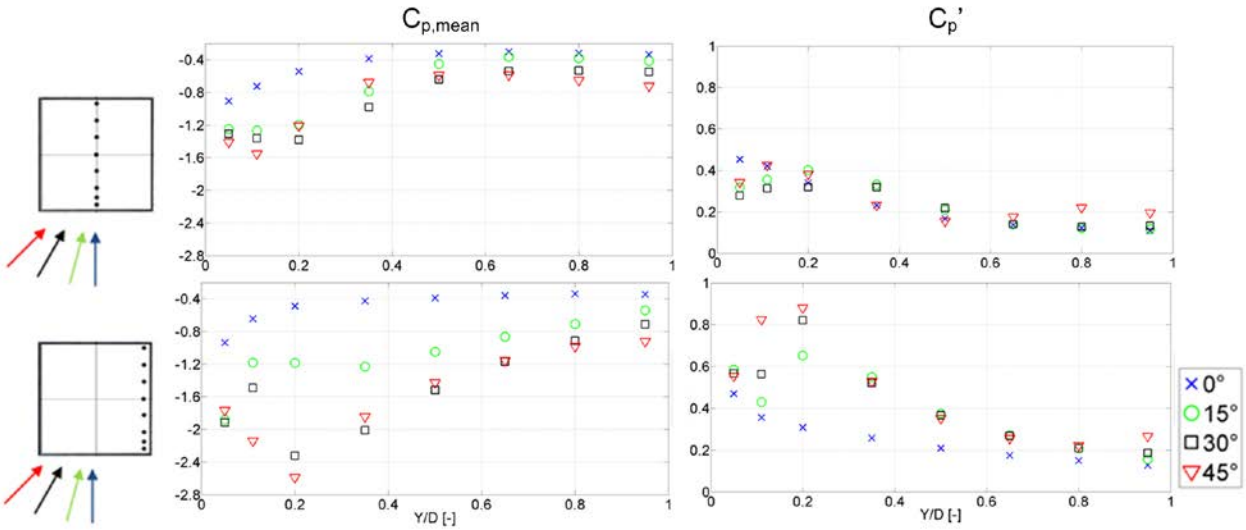

Fig. 5. Mean and standard deviation distribution of pressure coefficient along roof's middle line (up) and along roof's corner line at different wind angles (down).

3.2 Turbulence intensity

Fig. 6 provides a comparison of vertical profiles of stream-wise and vertical turbulence intensities (I_U and I_W, respectively) above the roof for different wind angles. For 0° wind angle, the turbulence intensity levels at higher positions above the roof top (from z/D=0.3) are quite high. In particular, when compared to the free-stream turbulence intensity at the reference model height (Fig. 1), notably higher turbulence intensities are measured being within the limits of 19-21% for I_U and 12.5-16.5% for I_W at height z/D=0.3. Observed flow behaviour can be explained by the configuration of the neighbouring buildings in a way that the incoming flow separates from the top of the upstream building and generates a shear flow that influence the flow over the principal building significantly. Figure 6 shows a significant reduction of turbulence intensities with height above the roof of the principal building.

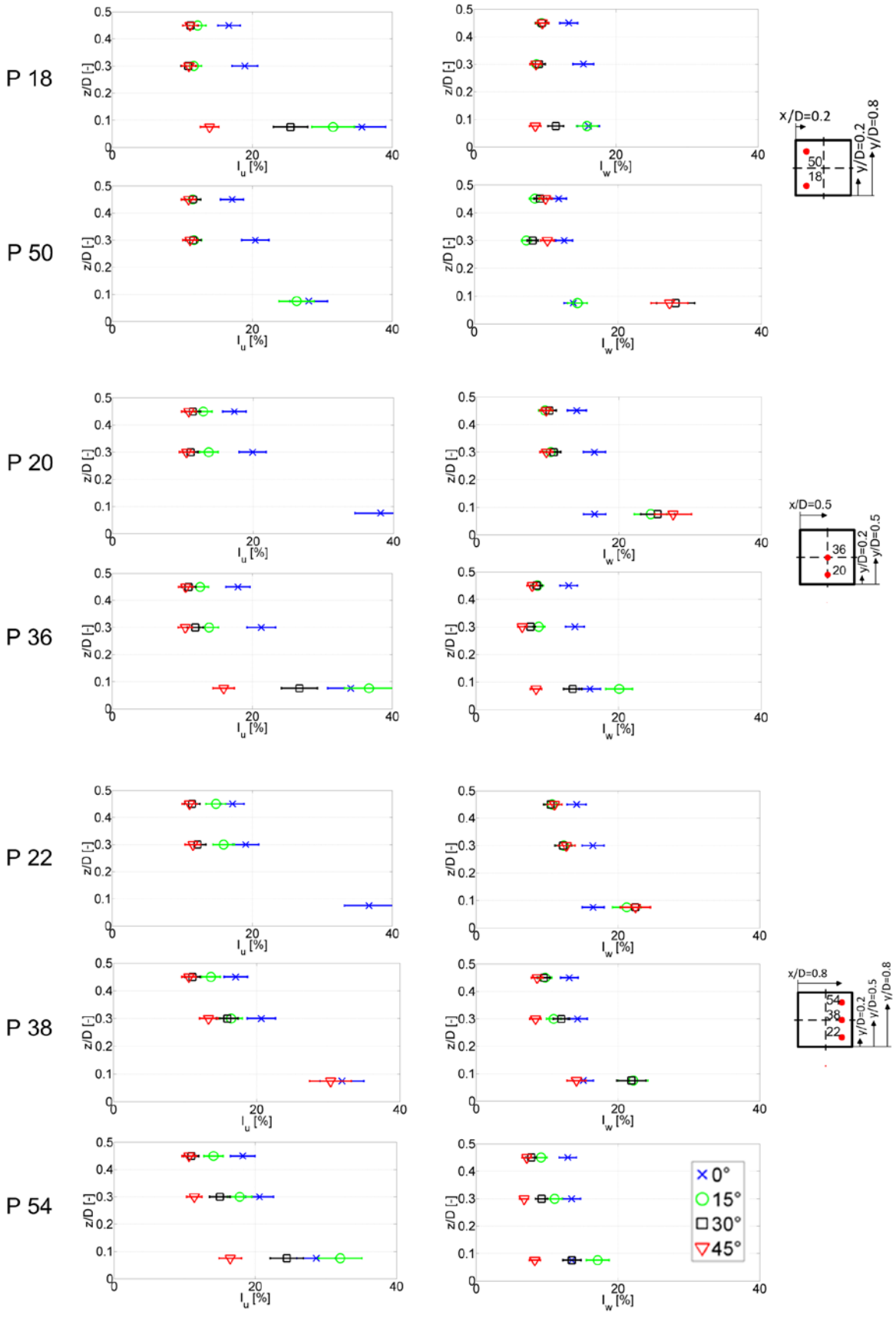
P 18
P 50
P 20
P 36
P 22
P 38
P 54
z/D [-]
I_u [%]
I_w [%]
x/D=0.2
y/D=0.2
y/D=0.8
50
18
x/D=0.5
y/D=0.2
y/D=0.5
36
20
x/D=0.8
y/D=0.2
y/D=0.5
y/D=0.8
54
38
22
0°
15°
30°
45°

1

Fig. 6. Stream-wise and vertical turbulence intensities with uncertainty limits measured above the points 18, 20, 22, 36, 38, 50 and 54 from Fig. 2.d)for wind directions: 0°, 15°, 30° and 45°. Measurement points with turbulence intensity over 40% are excluded due to a high level of uncertainty.

In contrast to 0°, the turbulence intensity levels for 15° wind direction are showing a zone of smaller turbulence intensities above the line x/D=0.2, i.e. above the points 18 and 50, that are more comparable to the reference free stream case. Namely, from the height of z/D=0.3 stream-wise intensity is around 11%, while it is around 7-9% for the vertical turbulence intensity. Those values are even slightly lower than the corresponding reference values. Nevertheless, higher turbulence intensities are recorded related to the flow above x/D=0.5, and even more significant increase is demonstrated in case of x/D=0.8, reaching up the values of I_U =15% at z/D=0.45. Owing to the geometrical configuration of 15° wind angle, it is possible that the shear flow generated from the upstream building is affecting the flow over this particular part of the principal building.

For most of the measurement positions, the turbulence intensity plots for 30° wind direction indicate that the flow from height z/D=0.3 is in accordance with the free stream flow. The exception is the flow above the points 38 and 54. Explanation of this turbulence intensity increase could be found in the flow pattern. Namely, Fig. 3 shows that point 38 is inside the separation cone, while the flow above point 54 might be influenced by the vortex shed from the upstream cones.

Similarly for 45° wind direction, the flow above the principal building seems to be not influenced by the flow from the upstream buildings. From the height z/D=0.3, the turbulence intensity is at the similar level as that of the free stream. Again, as in case of 15° and 30° wind direction existence of slightly lower values compared to the reference ones is observed. Only the flow above point 38, affected by the separation cone (Fig. 3), is showing slight increase in turbulence. Therefore, 45° wind direction is the most preferable direction concerning the turbulence.

However, in the vicinity of the roof at height z/D=0.075 the turbulence intensity of the stream-wise velocity component is above 20% for all considered wind angles. Nevertheless, the most favorable exception is 45° case and flow over point 18, where free-stream comparable values of turbulence intensities are measured.

3.3 Flow acceleration

To be able to compare the speed up effect above the roof, normalized velocity profiles above different measurement points for all considered wind angles are plotted on Fig. 7. The normalized local wind speed is evaluated as a ratio between mean stream-wise velocity and the mean reference velocity (U/U_{ref}). Similar normalization is also shown in Fig. 3. For 0° wind direction, a lack of a significant increase of wind speed over all considered points is observed. Namely, only from the height of z/D=0.45 a maximum increase compared to the referenced free stream velocity of around 10% is detected.

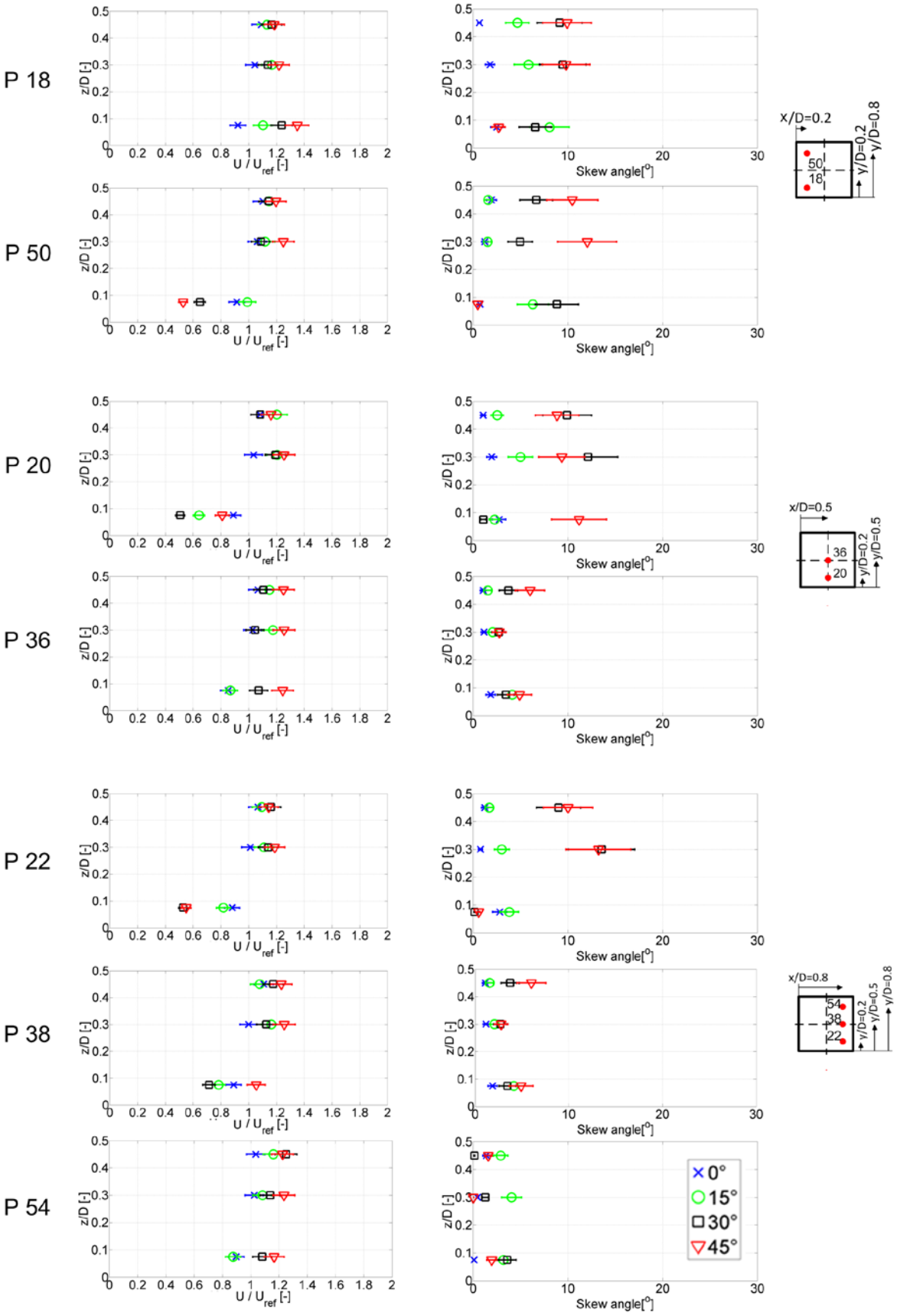
P 18
P 50
P 20
P 36
P 22
P 38
P 54
z/D [-]
U / U_ref [-]
Skew angle[°]
x/D=0.2
y/D=0.2
y/D=0.8
50
18
x/D=0.5
y/D=0.2
y/D=0.5
36
20
x/D=0.8
y/D=0.2
y/D=0.5
y/D=0.8
54
38
22
0°
15°
30°
45°

1

Fig. 7. Normalized stream-wise velocity (U/U_{ref}) and skew angle with uncertainty limits measured above the points 18, 20, 22, 36, 38, 50 and 54 from Fig. 2.d) for wind directions: 0°, 15°, 30° and 45°.

By contrast, increase of normalized velocity of around 16-17% is identified for 15° wind direction regarding several positions over the roof on even lower height of z/D=0.3. Maximum increase of 20% is detected above point 20. However, the region above the roof indicated in previous section as high turbulence region (flow over the line x/D=0.8) is characterized with lower normalized wind speeds.

It can be seen, that for 30° wind angle, the normalized velocities are mostly around 16-17% at the height z/D=0.45, but the maximum velocity increase is observed above the downstream point 54, reaching an increase of 25%.

Besides being the most favorable wind direction regarding the turbulence intensity levels, 45° wind direction is also indicating the highest increase of about 25% in stream-wise velocities at more than one location plotted in Fig. 7. One such example is the upstream point 50 in Fig. 3.d) that is positioned above the separation cone.

3.4 Skew angle

In this study the local velocity vector is calculated based on the two measured velocity components: stream-wise and vertical. As expected, very small skew angles are related to the flow above the roof at 0° wind angle (Fig. 7), due to the small value of the vertical component. Increasing the wind angle to 15° is followed by a slight increase of the skewed flow, related to the increase of the size of the separation region. Nevertheless, these measured values are still not exceeding 8%. On the other hand, for wind directions of 30° and 45°, significantly larger skew angles are recorded at some measurement points as shown in Fig. 7. Here, it is important to take into consideration large uncertainty bound of the measured skew angle. Namely, it is estimated at 25.8% following the same procedure from Section 2. Therefore, measured skew angles have to be considered more from a qualitative point of view. Yet, even the maximum recorded values including the uncertainty bounds, for wind directions of 30° and 45°, are well below the upper limit of attended angles in urban environment of 30° [6]. One such example is related to the flow above the point 22 for both angles of wind direction (30° and 45°) at the height of z/D=0.3 that is positioned above the separation region (Fig. 3.c) and 3.d)).

3.5 Effect of the neighboring buildings

Based on the presented results, 0° approaching wind angle seems to provide the most unfavourable conditions for wind energy harvesting, in contrast to 45° that can be regarded as the most desirable wind direction. To further explore such an observation, more detail measurements of the flow characteristics over the principal building are performed for both considered cases 0° and 45° wind angle, by measuring the velocities above the centre of the roof (middle point 36) at 10 heights and the results are presented in Fig. 8.a) and Fig. 8.b), respectively.

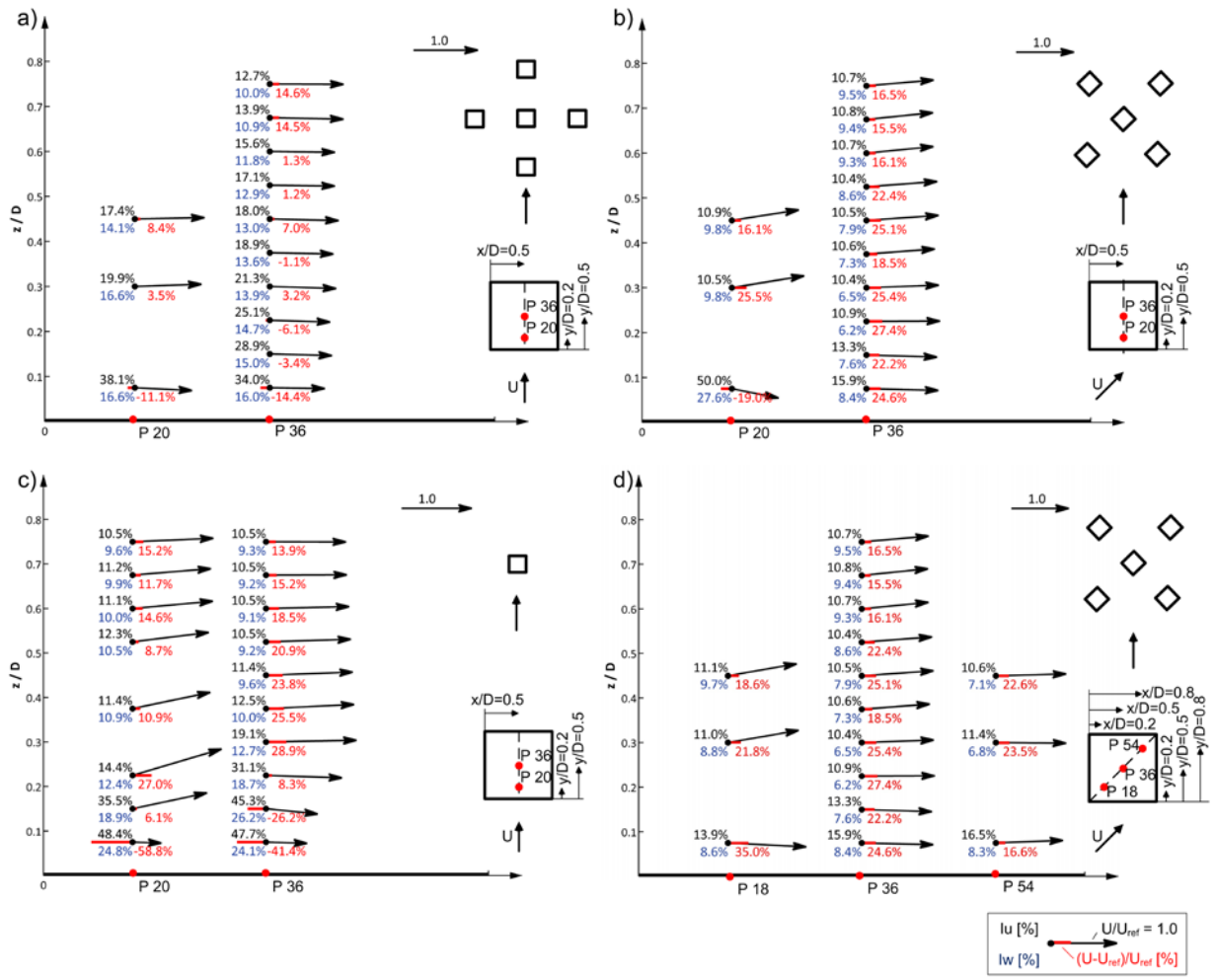

Fig. 8. Profiles of velocity vectors based on stream-wise and vertical velocity component, stream-wise turbulence intensity $I_{U,}$ vertical turbulence intensity I_W and percentage increase in the stream-wise wind speed. The legend linking the position of each value around the measurement point with its meaning indicates positions of : I_U - black number, marked left-up of the measurement point, I_W - blue number, marked left-down of the measurement point and percentage increase in the stream-wise wind speed - red number, marked right-down of the measurement point. Profiles over the principal high-rise building under the influence of 4 surrounding high-rise buildings are measured above points 20 and 36 (belonging to the marked line x/D=0.5) over the roof at: a) 0° angle, b) 45° angle, d) above the points 18, 36 and 54 (belonging to the marked stream-wise diagonal) at 45° angle; and c) over the single high-rise building above points 20 and 36 (belonging to the marked line x/D=0.5) at 0° angle [37]. The arrows indicate the velocity magnitude normalized with reference velocity (U_{ref}). Accompanying unity vector is represented in each plot.

For 0° wind angle, high turbulence intensity zone is detected to spread out through a notable area above the roof of the building. Namely, only above the height z/D=0.675 stream-wise and vertical turbulence intensities are becoming more comparable to the corresponding turbulence intensity levels of the referenced position in the free-stream. Therefore, the effect of this configuration - upstream building and the principal building downstream - on the turbulence intensity in the above roof flow is limited to a height of about two thirds of the building width.

In contrast to 0° case, 45° wind direction indicates substantially smaller turbulence intensities above the flat roof. High turbulence intensity region is detected only in the very near vicinity to the roof. Therefore, as from the height *z/D*=0.15, similar and even lower levels are detected compared to the referenced free stream case. In addition to the observed higher increase in the stream-wise wind velocity compared to 0°, flow above the point 36 indicates significant increase over a certain zone above the roof (Fig. 8.b). It is interesting to note, that part of these locations, detected as a speed-up region above the middle point 36, show an increase in the vertical velocity component (Fig. 8.b) at locations further away from the roof. The reason could be found in the incoming air that has to overcome the obstacle – the principal building – by lifting over the roof of the building. This can be supported by observing the flow over the stream-wise diagonal of the roof above the height *z/D*=0.3 (Fig. 8.d). Nevertheless, in this case small skew angles are detected, not exceeding 5%.

In order to further investigate the origin of observed flow characteristics, i.e. the influence of neighbouring buildings to the flow structure formed above the principal building, the comparison with the flow above geometrically similar structure, only isolated high-rise building, is performed. Study related to the flow above mentioned single high-rise building is also part of the COST TU1304 activities [28] and its results are presented in detailed in [37, 38]. This study takes into consideration same measurement strategy as presented in this work, including velocity and pressure measurements and same corresponding measurement points.

Geometrical arrangement of buildings in this work, under the 0° wind angle, suggest a possibility that the shear flow, developed due to separation from the top of the upstream building, influences the flow above the principal building. This is confirmed by a high level of turbulence intensity, measured above the roof. Besides having this negative effect on turbulence intensities, placing the building in between neighbouring arrangement causes a significant drop in normalized stream-wise wind velocity. It can be seen from Fig. 8.a) that only at positions from *z/D*=0.675 an increase in the stream-wise wind velocity is recorded and reached 14.5% of the value of the normalized stream-wise velocity. On contrary, flow above the single high-rise building accelerates reaching a significantly larger value of around 28.9% even at lower height above the middle point 36 (Fig. 8.c)). In addition, neighbouring buildings are affecting the flow pattern as well. Flow pattern presented in Fig. 8.c) clearly indicates the existence of large separation bubble developed above the roof of single high-rise building that is not the case with the flow above the principal building.

On the other hand, geometrical arrangement related to the 45° wind angle does not clearly indicate the cause of the observed flow characteristics. Namely, in such arrangement the upstream buildings do not overshadow the principal building as they have a projected distance of $D/\sqrt{2}$ to the principal building in the plane normal to the attack angle. This poses a question if this favourable wind characteristics are the result of the orientation of buildings at this angle or the flow above the principal building is only being unaffected by upstream buildings? Therefore, flow characteristics above the line *x/D*=0.8 of the principal building presented in Fig. 3. and repeated in Fig. 9.b) are compared with the flow above single high-rise building, presented in Fig. 9.a). Here, an important flow characteristic for wind harvesting - flow acceleration, is strongly pronounced by placing a building in the group arrangement. Higher levels of normalized stream-wise wind speed by order of two are measured above the principal high-rise building when compared to the flow above the single one. As for turbulence intensities, they are in the same range in both arrangements. This suggests that the shear layers developed from upstream buildings are not affecting the flow above the principal building. Based on the vector plots

presented in Fig. 9. in both arrangements separation cones are developed at upstream edges. Yet, placing a building in the group arrangement seems to lead to larger separation cone.

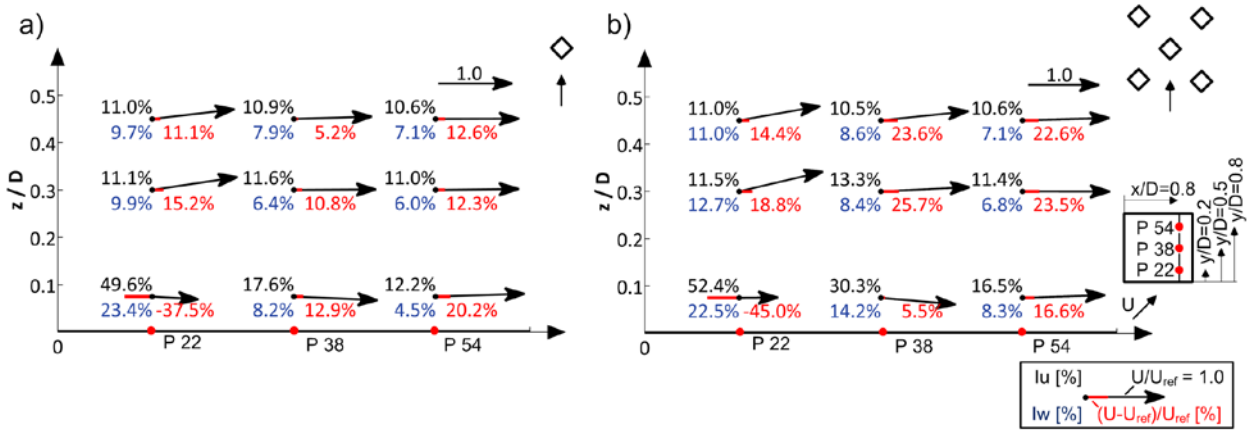

Fig. 9. Profiles of velocity vectors based on stream-wise and vertical velocity component, stream-wise turbulence intensity $I_{U,}$ vertical turbulence intensity I_W and percentage increase in the stream-wise wind speed. The legend linking the position of each value around the measurement point with its meaning indicates positions of : I_U - black number, marked left-up of the measurement point, I_W - blue number, marked left-down of the measurement point and percentage increase in the stream-wise wind speed - red number, marked right-down of the measurement point. Profiles measured above points 22, 38 and 54 (belonging to the marked line x/D=0.8) over the roof at 45° angle of: a) single high-rise building [38] and b) a principal high-rise building under the influence of 4 surrounding high-rise buildings (for comparison, results from Fig. 3. for 45° angle of attack are repeated). The arrows indicate the velocity magnitude normalized with reference velocity (U_{ref}). Accompanying unity vector is represented in each plot.

This more pronounced separation, related to the flow above the principle building placed in group arrangement, is confirmed by taking a look in pressure distribution over the roof. Fig. 10 shows the comparison of mean surface pressure coefficient of single high-rise building and principal building in group arrangement plotted along two symmetry lines at the roof. Even though both plots present the hump shapes related to conical vortex, as indication of larger separation, more pronounced hump shape is observed in the case of principal building in group arrangement. On contrary, placing a building in group arrangement for 0˚ wind angle leads to a reduction in the surface pressure.

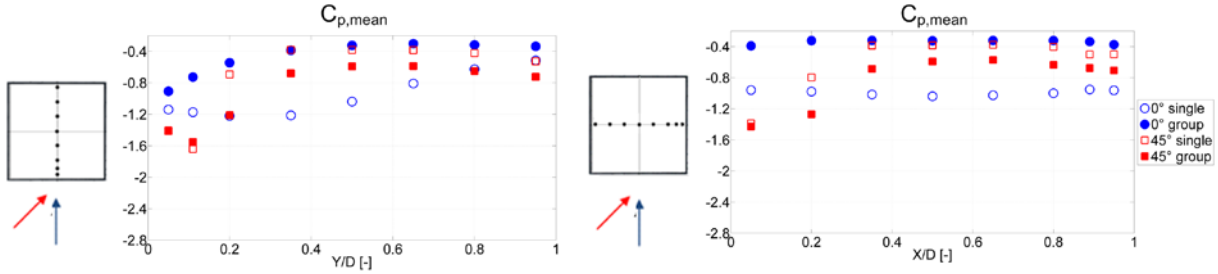

Fig. 10. Mean distribution of pressure coefficient along roof's middle lines- comparison between single arrangement presented in [38] and group arrangement for 0° and 45° approaching angle (for comparison, results from Fig. 5 for 45° angle of attack are repeated at the left plot).

As previously detected in Fig. 3. and Fig. 8. existence of regions with lower values of stream-wise and vertical turbulence intensity compared to reference free stream levels is observed. This is observed in Fig. 9. as well. Similar behavior is measured with Laser Doppler Anemometry (LDA 2-component system) in experiments reported in the CEDVAL database [39] above the stream-wise diagonal of a 45° rotated cube, where focus was on flow behavior and dispersion. In order to remove the influence of the speed-up effect of stream-wise velocity component from the evaluation of turbulence intensities (Eq. (1) and Eq. (2)), standard deviations of stream-wise and vertical velocity components of presented measurements are calculated and compared to the referenced free stream levels. This way, comparable or slightly higher values of standard deviation of stream-wise velocity components are obtained in mentioned regions above the roof. Yet, standard deviation of vertical velocity component in some regions above the roof is still slightly smaller compared to the free stream case, even including the uncertainty bounds. For example, this behavior is observed in the flow above the downstream point 54 in group arrangement in Fig. 9.b). Moreover, it exists in the single arrangement as well, above the points 38 and 54 in Fig. 9.a). Thus, the source of such behavior could be in the flow pattern. One possibility to establish the existence and actual cause of such regions could be to analyze the flow pattern by the use of validated numerical simulations.

Based on the above comments, it is clear that the influence of the orientation of the buildings for 45° approaching angle plays a significant role. However, the origin of such flow characteristics defers from shear layer effect detected in case of 0° approaching angle. One possibility is a passage effect, in a sense that the air passing between the models modifies the flow, in such manner that interacting with the upstream conical vortex increases the wind velocity of the vortex and enlarging the suction area. Similar flow behaviour is documented in [17] where the interference effect between two flat-roofed low-rise buildings is analyzed with a wind tunnel tests and noted that the suction area on the roof of the principal building is increased due to such passage effect.

Analyzing the flow in similar manner, i.e. by comparison with the flow above single high-rise building, flow characteristics related to other two yaw angles can be linked to previously detected effects. Namely, 15° approaching angle provides a flow pattern similar to 0° case, leading to the unwanted influence of the upstream building regarding wind energy harvesting. On the other hand, flow above principal building under 30° flow angle shows similarity to 45° case.

4 Conclusions

In this paper a wind tunnel investigation of the flow above the roof of a high-rise building surrounded by four similar high-rise buildings has been presented. The main idea was to obtain detailed representation of the flow characteristics with respect to the urban wind energy harvesting above high-rise buildings by joining the results of velocity and pressure measurements. Therefore, the presented results looked into the wind flow characteristics in terms of flow pattern, turbulence intensity, accelerated wind velocity and skew angle. Flat roof geometry was used in current investigation and the flow above it was considered for four different wind angles: 0°, 15°, 30°, and 45°. To analyze the influence of the neighboring buildings on the flow above the principle one, the flow pattern above the principal building was compared with the case of the flow above an isolated (single) high-rise building.

At 0° angle of the approaching flow, the shear layer is generated above the upstream building that significantly influences the flow above the principal building. A large area above the roof is

characterized by high levels of turbulence intensity and furthermore by lack of increase in the wind speed. Only from about two thirds of the building width above the roof this influence disappears. Yet, relatively small increase in wind speed compared to the reference level was obtained. This configuration is considered as the most unfavorable for wind energy harvesting.

The effect of the shear layer created from the upstream building has been recorded as well for the flow above the roof at 15° wind direction. Nevertheless, the unwanted influence of the upstream building is confined to a certain zone over the roof. Therefore, above created upstream separations, areas of lower turbulence intensity, as well as accelerated wind velocity exist, reaching a maximum increase of 20%.

For higher wind angles of, 30° and 45°, separation cones are generated at the upstream sides of the building. Yet, separation cones are more pronounced in case of the 30° flow angle. In these cases, relatively low turbulence intensity levels were observed, suggesting that the upstream shear layers are not penetrating the flow above the building. Maximum increase in the wind velocity of around 25% was recorded in both cases. The cause of such amplification could be the passage effect since the air is pushed to pass between the models of group arrangement. However, 45° wind direction is the most preferable wind direction, due to a large number of suitable locations over the roof top positioned as well at different heights.

Due to the large uncertainty bounds obtained in case of the skew angle, only some general tendencies can be pointed out. For smaller wind angles, small skew angles are also recorded. As for high angles of flow attack, in regions affected by the separation cones higher skew angles are recorded. Nevertheless, these values are in accordance with documented skew angles in urban areas.

This work presents a part of the database of the experimental urban wind benchmarks for validation of future CFD numerical investigations. In this manner more rigours extrapolation of the results will be obtained, with the aim of investigating in more detail relevant flow features around buildings and accessing the urban wind harvesting potential.

Acknowledgment

The authors would like to acknowledge the support provided by the COST-Action TU1304 – to sponsor the Short Term Scientific Mission in which this work was undertaken. The time and support received at the Ruhr-University Bochum by the Dr.-Ing. Christian Neuhaus and Mr. Ulf Winkelmann are also acknowledged.

References

[1] Lu L., Ip K.Y., 2009. Investigation on the feasibility and enhancement methods of wind power utilization in high-rise buildings of Hong Kong. Renewable & Sustainable Energy Reviews, 13, 450–461.

[2] Mayor of London: Action on Renewable Energy, http://www.london.gov.uk/mayor/environment/energy/renewable.jsp.

[3] Toja-Silva F, Colmenar-Santos A, Castro-Gil M., 2013. Urban wind energy exploitation systems: behavior under multidirectional flow conditions-opportunities andchallenges. Renew Sust Energy Rev, 24, 364–378.

[4] Walker SL., 2011.Building mounted wind turbines and the their suitability for the urban scale - a review of methods of estimating urban wind resource. Energy and Buildings, 43,1852–1862.

[5] Mertens S., 2006. Wind energy in the built environment, PhD thesis, Technical University Delft, Netherlands.

[6] Balduzzi F., Bianchini A., Ferrari L., 2012. Microeolic turbines in the built environment: Influence of the installation site on the potential energy yield, Renewable Energy, 45,163-174.

[7] Ledo L, Kosasih P.B., Cooper P., 2011, Roof mounting site analysis for micro-wind turbines. Renewable Energy 2011, 36, 1379–1391.

[8] Carpman N., Turbulence Intensity in Complex Environments and its Influence on Small Wind Turbines, Department of Earth Sciences, Uppsala University, Uppsala, 2011.

[9] Van Bussel G.J.W., Mertens S.M. Small wind turbines for the built environment. The Fourth European & African Conference on Wind Engineering (EACWE4), Prague, 11-15 July, 2005.

[10] Tsalicoglou, C., Barber, S., Chokani, N.,Abhari, R.S., 2012.Effect of flow inclination on wind turbine performance. Journal of Engineering for Gas Turbines and Power, 134.

[11] Balduzzi F, Bianchini A, Carnevale EA, Ferrari L, Magnani S. Feasibility analysis of a Darrieus VAWT installation in the rooftop of a building. In: Proceedings of the international conference on applied energy (ICAE).Perugia (Italy); 2011.

[12] Ahmad, S., Kumar, K., 2001. Interference effects on wind loads on low-rise hip roof buildings. Engineering Structures, 23, 1577–1589.

[13] Lam, K.M., Leung, M.Y.H., Zhao, J.G., 2008. Interference effects on wind loading of arow of closely spaced tall buildings. Journal of Wind Engineering and Industrial Aerodynamics 96, 562–583.

[14] Lam, K.M., Leung, M.Y.H., Zhao, J.G., 2009. Erratum to ’’Interference effects on wind loading of a row of closely spaced tall buildings’’. Journal of Wind Engineering and Industrial Aerodynamics 97, 110.

[15] Kim W., Tamura Y.,Yoshida A., 2011. Interference effects on local peak pressures between two buildings. Journal of Wind Engineering and Industrial Aerodynamics, 99, 584–600.

[16] Hui Y., Tamura Y., Yoshida A., 2012. Mutual interference effects between two high-rise building models with different shapes on local peak pressure coefficients. Journal of Wind Engineering and Industrial Aerodynamics, 104–106, 98–108.

[17] Pindado S., Meseguer J., Franchini S., 2011. Influence of an upstream building on the wind-induced mean suction on the flat roof of a low-rise building. Journal of Wind Engineering and Industrial Aerodynamics, 99, 889–893.

[18] Niemann, H.J., Köpper, H.D., 1998. Influence of adjacent buildings on wind effectson cooling towers. Engineering Structures, 20, 874–880.

[19] Khanduri A.C., Stathopoulos T., Bedard C., 1998. Wind-induced interference effects on buildings – a review of the state-of-the-art. Engineering Structures, 20, 617–630.

[20] Kawai H., 1997. Structure of conical vortices related with suction fluctuation on a flat roof in oblique smooth and turbulent flows. Journal of Wind Engineering and Industrial Aerodynamics, 69-71, 579-588.

[21] Kawai H., 2002. Local peak pressure and conical vortex on building. Journal of Wind Engineering and Industrial Aerodynamics, 90, 251-263.

[22] Kawai H., Nishimura G., 1996. Characteristics of fluctuating suction and conical vortices on a flat roof inoblique flow, Journal of Wind Engineering and Industrial Aerodynamics, 60 211-225.

[23] Banks D., Meroney R.N., Sarkar P.P., Zhao Z., Wu, F., 2000. Flow visualization ofconical vortices on flat roofs with simultaneous surface pressure measurement. Journal of Wind Engineering and Industrial Aerodynamics, 84, 65–85.

[24] Ono Y., Tamura T., Kataoka H., 2008. LES analysis of unsteady characteristics of conical vortex on a flat roof. Journal of Wind Engineering and Industrial Aerodynamics, 96, 2007-2018.

[25] Abohela I., Hamza N., Dudek S., 2013. Effect of roof shape, wind direction, building height and urban configuration on the energy yield and positioning of roof mounted wind turbines. Renewable Energy,50, 1106–1118.

[26] Toja-Silva F., Lopez-Garcia O., Peralta C., Navarro J., Cruz I. 2016. An empirical-heuristic optimization of the building-roof geometry for urban wind energy exploitation on high-rise buildings. Applied Energy, 164, 769–794.

[27] Al-Quraan A., Stathopoulos T., Pillay P. 2016. Comparison of wind tunnel and on site measurements for urban wind energy estimation of potential yield. Journal of Wind Engineering and Industrial Aerodynamics, 158, 1-10.

[28] COST Action TU1304, WINd Energy Technology Reconsideration to Enhance the Conceptof Smart Cities (WINERCOST). Available online: http://www.winercost.com/

[29] Jorgensen, F., 2004. How to measure turbulence with hot-wire anemometers – a practical guide, Dantec Dynamics, Denmark.

[30] Yavuzkurt, S., 1984. A Guide to Uncertainty Analysis of Hot-Wire Data, ASME, J. Fluids Engr., Vol. 106.

[31] Neuhaus, C., 2010. Numerische frequenzabhängige Kalibrierung langer Druckmessschlauchsysteme. Internal Report, Wind Engineering and Flow Mechanics, Ruhr-Universität Bochum, Germany.

[32] Hunt A., 1982. Wind-tunnel measurements of surface pressures on cubic building models at several scales, Journal of Wind Engineering and Industrial Aerodynamics, vol. 10, 137-163.

[33] Tieleman H. and Akins R., 1996. The effect of incident turbulence on the surface pressures of surface-mounted prisms, Journal of Fluids and Structures, vol. 10, 367-393.

[34] Kray T., Paul J., 2017. Peak negative pressure coefficient on low-tilted solar arrays mounted on flat roofs: the effect of the building size and model scale**,** Proceedings of European-African Conference on Wind Engineering (EACWE), 4-7. July, Liege, Belgium.

[35] Šarkić Glumac, A., Hemida, H., Höffer, R.. 2017. Wind tunnel experimental data for flow characteristics above the roof of high-rise buildings in group arrangement for wind energy harvesting, Mendeley Data, v2, http://dx.doi.org/10.17632/cxc4w2myyw.2

[36] Haan F.,2000. The effects of turbulence on the aerodynamics of long-span bridges, PhD thesis, University of Notre Dame, Indiana.

[37] Hemida, H., Šarkić, A., Gillmeier, S., Höffer, R. 2015. Experimental investigation of the wind flow above the roof of a high-rise building, WINERCOST Workshop ‘Trends and Challenges for Wind Energy Harvesting‘, Coimbra, Portugal.

[38] Hemida, H., Šarkić Glumac, A., Höffer, R.. On the Flow above the Roof of High-Rise Buildings for Wind Energy Harvesting, Journal of Wind Engineering and Industrial Aerodynamics (paper submitted in this issue).

[39] EWTL, Environmental Wind Tunnel Laboratory, M. I. H. U., May 2017. Compilation of experimental data for validation of microscale dispersion models (cedval). URL http://www.mi.zmaw.de/index.php?id=433